Journal of Applied Physics

RESEARCH ARTICLE | APRIL 18 2014

Hydride vapor phase epitaxy and characterization of high-quality ScN epilayers

Yuichi Oshima; Encarnación G. Víllora; Kiyoshi Shimamura

J. Appl. Phys. 115, 153508 (2014)
https://doi.org/10.1063/1.4871656

Hydride vapor phase epitaxy and characterization of high-quality ScN epilayers

Yuichi Oshima,[a] Encarnación G. Víllora, and Kiyoshi Shimamura
Environment and Energy Materials Research Division, National Institute for Materials Science, 1-1 Namiki, Tsukuba, Ibaraki 305-0044, Japan

(Received 7 March 2014; accepted 3 April 2014; published online 18 April 2014)

The heteroepitaxial growth of ScN films was investigated on various substrates by hydride vapor phase epitaxy (HVPE). Single crystalline mirror-like ScN(100) and ScN(110) layers were successfully deposited on r- and m-plane sapphire substrates, respectively. Homogeneous stoichiometric films (N/Sc ratio 1.01 ± 0.10) up to 40 μm in thickness were deposited. Their mosaicity drastically improved with increasing the film thickness. The band gap was determined by optical methods to be 2.06 eV. Impurity concentrations including H, C, O, Si, and Cl were investigated through energy dispersive X-ray spectrometry and secondary ion mass spectrometry. As a result, it was found that the presence of impurities was efficiently suppressed in comparison with that of HVPE-grown ScN films reported in the past, which was possible thanks to the home-designed corrosion-free HVPE reactor. Room-temperature Hall measurements indicated that the residual free electron concentrations ranged between 10^{18}–10^{20} cm^{-3}, which was markedly lower than the reported values. The carrier mobility increased monotonically with the decreasing in carrier concentration, achieving the largest value ever reported, 284 cm^2 V^{-1} s^{-1} at $n = 3.7 \times 10^{18}$ cm^{-3}. © *2014 AIP Publishing LLC*. [http://dx.doi.org/10.1063/1.4871656]

I. INTRODUCTION

ScN is a group III transition metal nitride semiconductor, which crystallizes in the cubic rock-salt crystal structure with a lattice constant of 4.505 Å.[1] Similar to other transition metal nitrides, ScN exhibits excellent physical properties, such as high hardness and high thermodynamic stability, which are comparable to those of TiN.[1–3] ScN is reported to have a direct band gap of 2.1–3.2 eV, and an additional indirect band gap of 0.9–1.3 eV has been predicted.[3–5] Since ScN(111) lattice matches to wurtzite-GaN(0001) and cubic-GaN(111), it has been used as a buffer layer or interlayer to reduce the threading dislocation density in GaN epilayers.[6–9] In addition, $Ga_xSc_{1-x}N$ alloys[10–16] and the ScN/GaN hetero-junction[17] are being investigated to improve the performance of GaN-based devices. Furthermore, among the transition metal nitrides, ScN possesses an anomalous high thermoelectric factor,[18,19] which make it potential candidate material for high temperature thermoelectric applications. ScN is also promising as a host material of ferromagnetic semiconductors due to its high manganese solubility and an estimated high Curie temperature.[20,21] $Al_xSc_{1-x}N$ alloys shows an exceptionally large piezoelectric response,[22,23] and meta-stable hexagonal ScN is expected to have even greater piezoelectric constant, comparable to that of ferroelectric perovskites.[24] ScN is thus a very attractive material, which has a great potential for various applications.

The growth of ScN thin film has been investigated mainly by molecular beam epitaxy (MBE), sputtering, and hydride vapor phase epitaxy (HVPE). The growth temperature is below 900 °C in most of the cases. The typical growth rate is below 0.5 μm/h, and the film thickness is usually below 1 μm except the case of HVPE. Although there are no lattice-matched substrate materials, the growth of single crystalline ScN films has been reported on sapphire, MgO, and Si.[25–32] In general, heteroepitaxial growth on highly lattice-mismatched substrates leads to significant mosaicity, involving high density of crystal defect such as dislocations. There are a few reports on the structural quality of ScN films,[27,30] and the best reported FWHM of X-ray rocking curve is 0.35°, which is still far from the quality of conventional, high quality semiconductors, such as Si, GaAs, and GaN. On the other hand, in order to use semiconductors in device applications, generally their conduction type and carrier concentration need to be controlled precisely. In the case of ScN, however, such control has not been realized yet. Nominally un-doped ScN usually shows strong n-type conduction, with a high residual carrier concentration ranging between 10^{19} to 10^{22} cm^{-3}.[29–32] The plausible origins of the donors are impurities and crystal defects such as nitrogen vacancies. However, their contribution has not been fully clarified in detail yet. In order to exploit the full potential of ScN and to pave the road to practical use, it is essential to clarify and control the effect of crystal defects and impurities by the growth of high-quality and high-purity crystals.

In this work, we have employed HVPE as the growth technique of ScN. HVPE is a kind of chemical vapor deposition (CVD) technique, which was first reported by Tietjen and Amic in 1966 as a growth method of III-V semiconductors such as GaAsP.[33] Nowadays, HVPE is widely used for the mass production of freestanding GaN single crystal wafers.[34,35] The method is characterized by a fast growth rate and the high crystalline quality of resulting layers. Usually, the equilibrium constant of HVPE is far smaller than those of MBE and metalorganic vapor phase epitaxy (MOVPE). Such small equilibrium constant allows one to

[a]Electronic mail: OSHIMA.Yuichi@nims.go.jp

supply high concentration gaseous source materials to realize a high growth rate without parasitic gas phase reaction. In addition, such small equilibrium constant enables the crystal to grow under nearly thermal equilibrium condition, which leads to the growth of high quality crystals.

The first HVPE of ScN was reported by Dismukes *et al.* in 1970.[31,32] They demonstrated the epitaxial growth of ScN on r-plane sapphire substrate within 850–930 °C. Besides this temperature range, all samples were polycrystalline. The single crystalline growth was possible at growth rates below 2.8 μm/h, and relatively thick films up to 20 μm were obtained. Their nominally un-doped ScN films also showed n-type conductivity with high carrier concentrations in the order of 10^{20}–10^{21} cm^{-3}, which are comparable to those of ScN films grown by MBE or sputtering. Their ScN films contained chlorine and oxygen impurities in high concentrations, i.e., $[Cl] = 1.8 \times 10^{20}\,cm^{-3}$ and $[O] = 4.4 \times 10^{19}\,cm^{-3}$, respectively. The high carrier concentration was attributed to the presence of Cl ions, because their concentrations were comparable. In spite of such high carrier concentration, the carrier mobility was also relatively high, 151 $cm^2\,V^{-1}\,s^{-1}$ at $n = 1.1 \times 10^{20}\,cm^{-3}$, which is twice as high as that of silicon.

In recent years, Edger *et al.* tried to grow ScN on 6 H-SiC substrates by HVPE.[36] Their ScN films contained aluminum and chlorine as impurities in much higher concentrations, being even detectable by energy dispersive X-ray spectrometry (EDX). In this case, the Al impurity was assumed to originate from the reaction between the scandium-chloride reactant and an alumina tube used to contain Sc metal in the HVPE reactor. The [Al] was as high as 1.5 at. % in their ScN film grown at 1000 °C. By decreasing the temperature of the alumina tube (source temperature) from 1000 to 800 °C, the corrosion was suppressed and [Al] decreased. However, [Al] was still high (~0.5 at. %) and [Cl] increased from 1.9 to 2.7 at. % due to the diminished Cl desorption from the growth front.

As stated above, ScN is a very attractive material, and it is necessary to realize high quality epilayers with well-controlled electrical conductivity for device applications. HVPE is, in principle, a promising growth method for ScN. However, this technique needs to be improved in order to avoid the incorporation of impurities into the films, which is caused by the chamber corrosion with the highly reactive source materials. In this work, we demonstrate the growth of high-quality, high-purity ScN epilayers by using an originally developed corrosion-resistant HVPE reactor. The crystalline, optical, and electrical properties of the resulting ScN films are analyzed and discussed.

II. EXPERIMENTAL METHOD

A. HVPE growth of ScN

Generally, quartz and alumina are the principal materials to construct a HVPE reactor. However, as was stated in the former section, these materials are corroded by scandium and scandium chloride, the source materials of ScN in HVPE.[37,38] Therefore, we have designed our own home-made HVPE reactor avoiding the use of quartz and alumina in the high-temperature zone. The structure of the reactor is schematically shown in Fig. 1. A water-cooled quartz tube is employed as the outer tube. Inside, a pBN-coated graphite tube is coaxially located. The graphite tube is inductively heated by an RF-coil around the quartz tube to create a hot zone inside. Between both quartz and graphite tubes, there is a pBN tube radiation shield, which prevents the overheating of the inner quartz wall. Ar-gas is purged to avoid the exposure of the inner quartz wall to the corrosive materials. Inside the graphite tube, the inner flow channel, the substrate holder, and the Sc container are composed of corrosion-resistant materials, such as tungsten and SiC.

ScN was grown in the home-made HVPE reactor at atmospheric pressure using scandium chloride and NH_3 (99.9999% pure) as source materials. No intentional doping was carried out. Scandium chloride was formed upstream in the reactor by the reaction between solid Sc metal (99.99% pure) and HCl gas (99.999% pure). The partial pressures of the HCl (P_{HCl}) and NH_3 (P_{NH3}) were varied between 0.124–1.24 kPa and 6.2–19.3 kPa, respectively. The saturated vapor pressure of $ScCl_3$, one possible product formed by the reaction between Sc and HCl, reaches 100 kPa at 1037 °C.[39] Therefore, in order to prevent the condensation of $ScCl_3$, the temperature of the reactor was kept constant at a bit higher value 1050 °C. Usually, nitrogen gas is used as a carrier gas in HVPE. However, N_2 and Sc react directly with each other to form ScN at high temperatures.[40] Instead of N_2, we employed Ar as carrier gas.

We have also investigated which substrates are appropriate for the heteroepitaxial growth of ScN. Sapphire, MgO, Yttrium-stabilized zirconia (YSZ), GaN, and AlN were taken under consideration. In this investigation, P_{HCl} and P_{NH3} were fixed to be 0.31 kPa and 10.6 kPa, respectively. All depositions were carried out at 1050 °C for 5 min using the same growth recipe. The ScN films were directly grown on each substrate without any buffer layer to compensate for lattice mismatch.

B. Characterization methods

The crystal orientation of HVPE-grown ScN films was investigated by X-ray diffraction ω-2θ scan and pole figure measurements. The surface morphology was observed by means of Nomarski microscopy and scanning electron microscopy (SEM). The growth rate was determined by cross-sectional SEM. The N/Sc composition ratio and concentrations of impurities were estimated by Rutherford backscattering spectrometry (RBS), EDX, and secondary ion

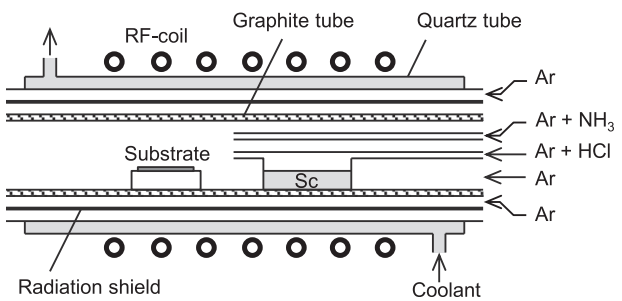

FIG. 1. Schematic of the HVPE reactor used for ScN growth.

mass spectrometry (SIMS). The mosaicity (tilt and twist) in the films was evaluated through X-ray rocking curve measurements in symmetric and skew-symmetric geometry. Transmittance and reflectance spectra were utilized to figure out the optical absorption coefficient and to determine the optical band gap. Electrical properties (carrier concentration and electron mobility) were investigated by Hall measurements by the van der Pauw method. All the measurements were carried out at room temperature.

III. RESULTS AND DISCUSSION

A. Chemistry of ScN growth

First of all, we discuss the chemical reactions by which ScN is produced by HVPE. Dismukes *et al*. studied the vapor phase reactions involved in ScN HVPE.[32] They presumed that $ScCl_2$ is the predominant scandium chloride species since only a dihalide is generated in the case of chemical reaction between Cl_2 and Y, being chemically similar to Sc.

In our case, however, the predominant scandium chloride species would be $(ScCl_3)_x$, since the molar ratio of the supplied HCl and the decrease of Sc metal was 3:1. According to Patrikeev *et al*., $ScCl_3$ and Sc_2Cl_6 co-exist in thermal equilibrium,[39] and approximately 74% should be Sc_2Cl_6 at our reactor temperature 1050 °C. Therefore, we presume that following reactions are taking place simultaneously:

$$Sc_2Cl_6 + 2NH_3 = 2ScN + 6HCl,$$

$$ScCl_3 + NH_3 = ScN + 3HCl.$$

B. Investigation of substrates for heretoepitaxy of ScN

Table I summarizes the results of ScN growth on various substrates. Films grown on MgO, YSZ, GaN were peeled off and broke into pieces after deposition. This behavior is attributed to a substrate etching process at the interface, probably related to the presence of HCl gas in the growth atmosphere.

Mechanically stable films were successfully grown on sapphire and AlN. X-ray ω-2θ scan (not shown) revealed that the ScN films grown on c- and a-plane sapphire and AlN included domains with mixed out-of-plane orientations of (100) and (111). ScN films with single out-of-plane orientation were obtained on r- and m-plane sapphires, i.e., $(100)_{ScN}//(10\text{-}12)_{sap}$ and $(110)_{ScN}//(10\text{-}10)_{sap}$, respectively. Figures 2(a) and 2(b) are the X-ray pole figures of the ScN(100) and the ScN(110) films. The pole figure of the ScN(100) film shows (111) poles with four-fold symmetry, and that of the ScN(110) film shows (200) poles with two-fold symmetry as expected for single in-plane orientation films. This proves that single crystalline films were achieved on r- and m-plane sapphire. From the ϕ-scan profiles of the epilayers and the substrates (not shown), following epitaxial relationships were elucidated:

$$\text{ScN on r-plane sapphire}: (100)_{ScN}//(10-12)_{sap} \text{ and } [001]_{ScN}//[11-20]_{sap},$$

$$\text{ScN on m-plane sapphire}: (110)_{ScN}//(10-10)_{sap} \text{ and } [001]_{ScN}//[11-20]_{sap}.$$

In the following, the characterization of these single crystalline films is described.

C. Growth rate of ScN

Figure 3 shows the growth rate of ScN as a function of (a) P_{HCl}, and (b) P_{NH3}. The results of ScN(100) and ScN(110) were identical within the thickness accuracy estimated by SEM. The growth rate first increases with increasing P_{HCl}, reaches maximum around $P_{HCl} = 0.5$ kPa, and then starts to decrease. The dependence on P_{NH3} is similar. The decrease in growth rate probably results from a gas-phase reaction upstream in the reactor that consumes scandium chloride and NH_3 before they arrive at the substrate.

The next sections present and discuss the morphological, structural, optical, and electrical properties of ScN films grown under representative growth condition, $P_{HCl} = 0.31$ kPa and

TABLE I. Results of HVPE growth of ScN on various substrates.

Substrate		Result
Sapphire	c-plane (0001)	Mixed orientations, (100) and (111)
	a-plane (11–20)	
	m-plane (10–10)	(110) single crystalline
	r-plane (10–12)	(100) single crystalline
MgO	(100)	Chemically unstable
	(110)	
YSZ[a] (100)		
GaN, c-plane (0001)		
AlN, c-plane (0001)		Mixed orientations, (100) and (111)

[a]Y_2O_3 (10 mol. %)—ZrO_2 (90 mol. %)

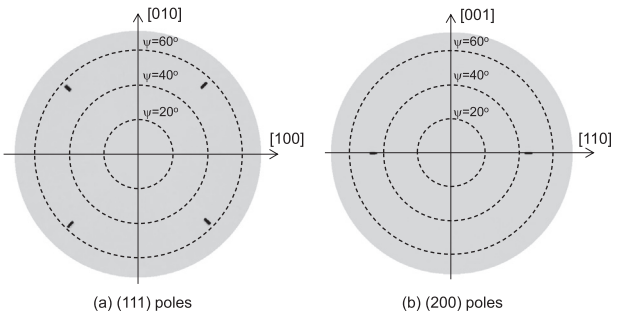

FIG. 2. X-ray pole figures of ScN films grown on (a) r-plane sapphire and (b) m-plane sapphire.

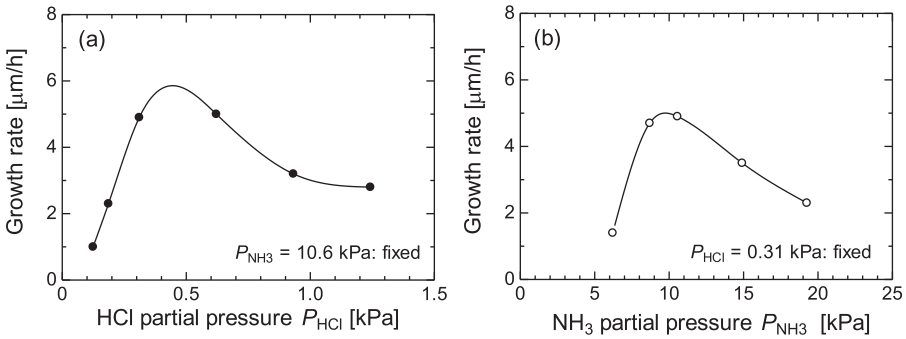

FIG. 3. Growth rate of ScN as a function of (a) HCl partial pressure, (b) NH_3 partial pressure.

$P_{NH3} = 10.6$ kPa, corresponding to a growth rate of $\sim 5\ \mu$m/h. The growth time was varied from 5 min to 8 h, thus the thickness ranged approximately between $0.4 \sim 40\ \mu$m.

D. Surface morphology of HVPE-grown ScN

The surface of all the samples was mirror-like for human eyes. Figures 4 and 5 show surface Nomarski microscope images and SEM images (bird's eye view) of the HVPE-grown ScN films. On the surface can be observed hillocks, whose averaged diameter increases with the layer thickness. As it will be seen in Sec. III E, the crystalline quality of the ScN films improves with increasing film thickness. So, if theses hillocks are reflecting the sub-grain structure of the mosaic films, this increase in hillock size, i.e., decrease in the density of hillocks, agrees well with the improvement of the structural quality.

In SEM images of Fig. 5, ScN(100) surface appears smoother than ScN(110). This can be explained by the difference in the surface diffusion barrier, which arises from the number of dangling bonds. In the case of ScN(100) surface, each atom will have only a single dangling bond, whereas each atom of ScN(110) surface will have two dangling bonds. Therefore, the surface diffusion barrier of ScN(100) should be lower than that of ScN(110). An analogous argument is found in the comparison of MBE-grown ScN(100) and ScN(111) surfaces.[3] Our films, both ScN(100) and ScN(110), exhibit a much smoother surface compared to the HVPE-grown ScN films reported by Dismukes *et al.* and Edger *et al.*[32,36] This fact can also be explained from the view point of surface diffusion barrier. The ScN films of Dismukes *et al.* and Edger *et al.* had surfaces of ScN(321) and ScN(111), respectively. On the both planes, each atom has three dangling bonds and hence the surface diffusion barrier should be higher than those of ScN(100) and ScN(110). In addition, our growth temperature is substantially higher than those of the previous reports. Therefore, it is plausible that such a high growth temperature favors the surface diffusion, resulting thus in a smoother surface.

E. Structural properties

Figures 6(a) and 6(b) show the thickness dependences of tilt and twist angles of our HVPE-grown ScN films. In the case of ScN(100) films, we use the FWHMs of (200) and (131) rocking curves as the measure of the out-of-plane and in-plane mosaicity, i.e., tilt and twist angles, respectively. Analogously, we employed the FWHMs of (220) and (-240) reflections as tilt and twist angles for ScN(110) films. Both (131) and (-240) are inclined from the film surface by approximately 72°.

The tilt and twist angles monotonically decreased with increasing film thickness. A similar quality improvement has

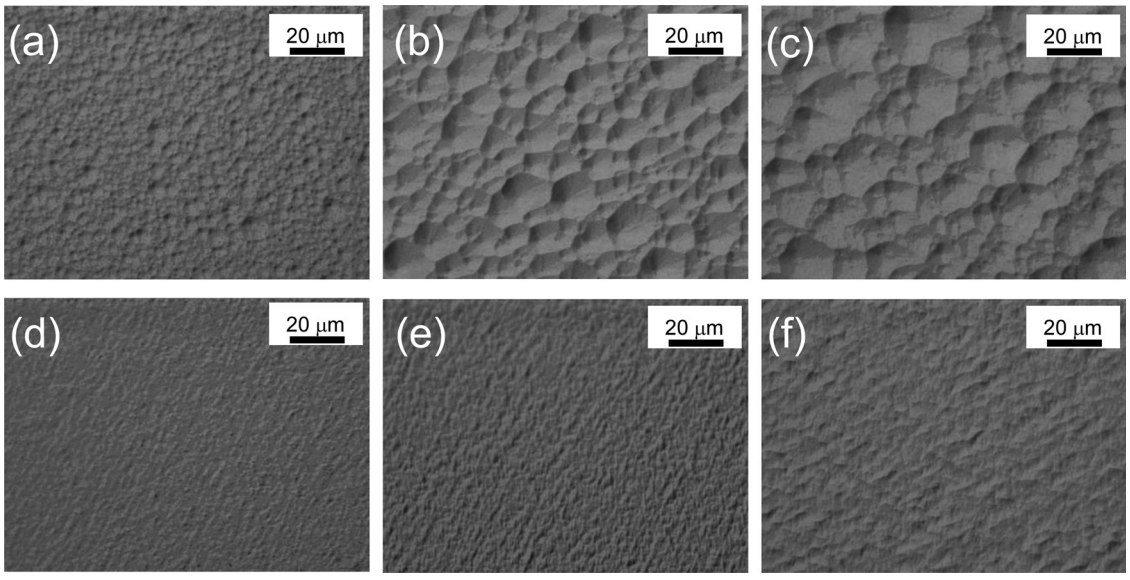

FIG. 4. Nomarski microscope surface images of: ScN (100) films with an approximate thickness of (a) 10 μm, (b) 20 μm, (c) 40 μm ScN (110) films with an approximate thickness of (d) 10 μm, (e) 20 μm, (f) 40 μm.

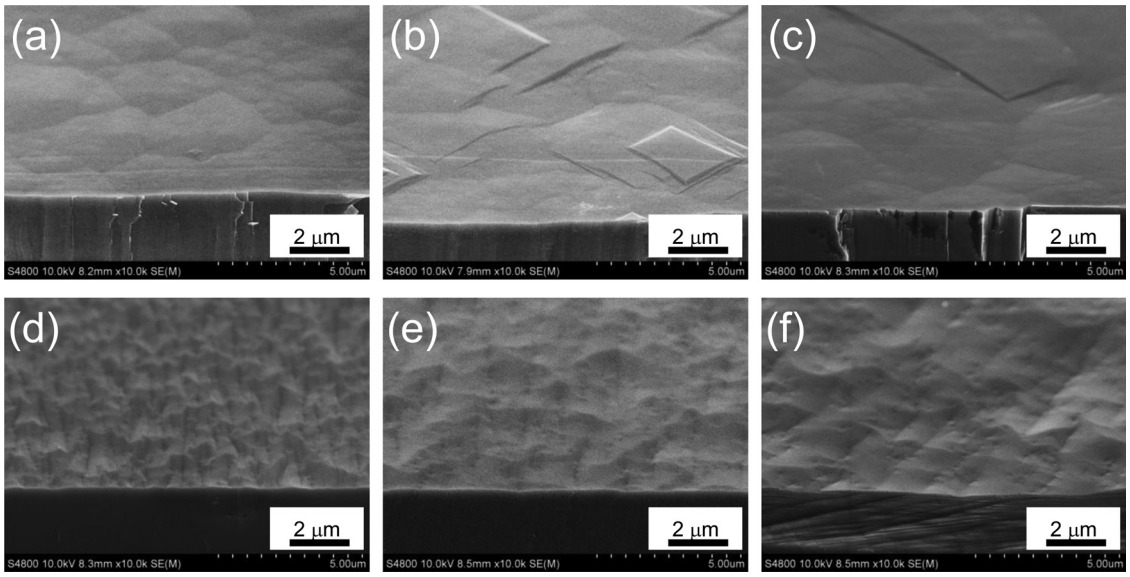

FIG. 5. SEM images (bird's eye-view) of: ScN (100) films with an approximate thickness of (a) 10 μm, (b) 20 μm, (c) 40 μm ScN (110) films with an approximate thickness of (d) 10 μm, (e) 20 μm, (f) 40 μm.

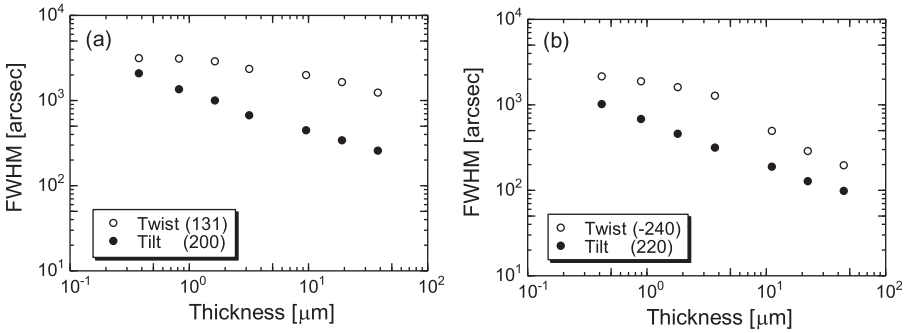

FIG. 6. Thickness dependence of XRC-FWHM of (a) ScN (100) and (b) ScN (110).

been observed in the case of GaN films. The interpretation given to this phenomenon is that dislocations with opposite Burgers vector gradually approach each other due to the attractive interaction between them, and then react with each other to make a dislocation loop during thick film growth.[41] The same mechanism would be possible in the case of ScN. In order to confirm this, it will be necessary to perform the direct observation of dislocations by cross-sectional TEM.

We have also found that ScN(110) films have a better quality than ScN(100) ones when their thickness is the same. The lattice mismatch between m-plane sapphire and two periods of ScN(110) along $[1\text{–}10]_{ScN}$ is 2%, while that between r-plane sapphire and three periods of ScN (100) along $[010]_{ScN}$ is 14%. The difference in the structural quality is likely to be originated from this difference in lattice match.

F. Optical properties

Figure 7(a) shows the transmittance (T), the reflectance (R), and the absorption coefficient (α) of a ScN(110) film (3.7 μm thick) as a function of photon energy ($h\nu$). Both T and R show a clear oscillation due to the multiple reflections on both sides. α was estimated from T and R by the method described elsewhere.[42] α shows a steep increase around 2.1 eV. No threshold was observed around 0.9–1.3 eV, where the existence of the indirect transition is predicted. It should be noted that the apparent α saturation above 2.1 eV is an

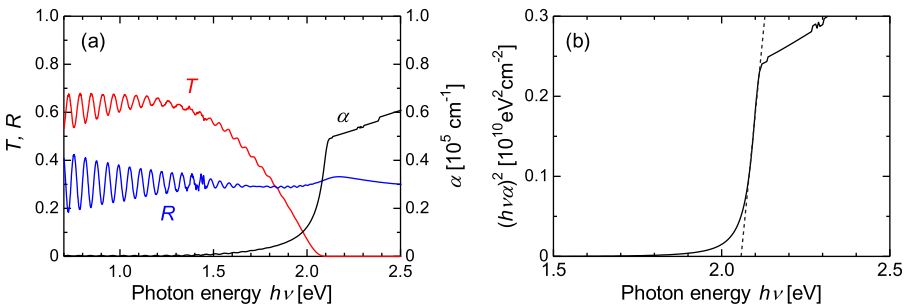

FIG. 7. (a) Transmittance and reflectance spectra of ScN (110), (b) Absorption coefficient in $(h\nu\alpha)^2$ vs $h\nu$ plot.

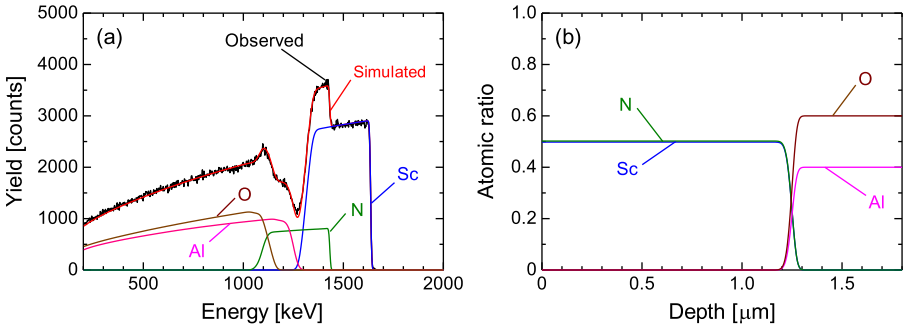

FIG. 8. (a) RBS spectrum of ScN (100), (b) depth profile of atomic ratio of Sc, N, Al, O.

experimental artifact caused by the decrease in transmittance signal below the detection limit of our instrument for the relatively large film thickness. Therefore, α should be greater in reality. Figure 7(b) is the absorption coefficient spectrum in $(h\nu\alpha)^2$ vs $h\nu$ plot. The linear range correlates clearly with the direct transition, and the band gap energy was determined to be 2.06 eV by a linear fit. The data for ScN(100) films (not shown) show no significant difference with the results of ScN(110) films.

The direct band gap of ScN is reported to lie in the range of 2.1–3.2 eV. Our band gap corresponds with the minimum reported values. Moram *et al*. have demonstrated that oxygen contamination leads to an increase in the direct band gap energy of ScN.[43] Therefore, our small energy gap is indicative of a low oxygen contamination in our samples. Indeed, the oxygen concentration is found by SIMS to be in the order of $10^{17}\,\mathrm{cm}^{-3}$, as it will be seen in Sec. III G.

G. Composition and impurity concentration

We have investigated the N/Sc composition ratio of 1.2-μm-thick ScN(110) film by RBS using H^+ and $^4He^+$ as incident ions. Nitrogen sensitive measurements are possible when H^+ is utilized, while $^4He^+$ enables high depth resolution measurements. Figure 8(a) shows the RBS spectrum obtained with H^+ as incident ion. The spectrum was accurately reproduced by assuming the existence of only Sc, N, Al, and O, i.e., no impurity was observed by RBS. The estimated N/Sc ratio from this spectrum is 1.01 ± 0.10. Therefore, no significant deviation from the stoichiometric ratio (N/Sc = 1) was observed. Figure 8(b) is the depth profile of the composition calculated from the RBS spectrum (not shown) obtained with $^4He^+$ as incident ion. The N/Sc ratio was confirmed to be stoichiometric along the depth direction within the RBS accuracy.

No element except Sc and N was detected by EDX. In order to obtain more detailed information about potential impurities (namely H, Cl, C, O, Si, and W), SIMS was carried out. H and Cl are contained in HCl and NH_3 gases. C, O, Si, and W are constituents of the HVPE reactor materials. As a result, all the elements except W were detected. Figure 9 shows the depth profile of the SIMS measurement. The present [C] and [O] are approximately $7.9 \times 10^{17}\,\mathrm{cm}^{-3}$ and $8.8 \times 10^{17}\,\mathrm{cm}^{-3}$, respectively. Even though these concentrations are significant, these are remarkably lower than those reported by Dismukes *et al*., with $[C] = 1.7 \times 10^{19}\,\mathrm{cm}^{-3}$ and $[O] = 4.4 \times 10^{19}\,\mathrm{cm}^{-3}$.[32] In the case of Si, there is no report on ScN, and our value $[Si] = 1.6 \times 10^{16}\,\mathrm{cm}^{-3}$ is comparable to that of HVPE-grown GaN. Regarding [H] and [Cl], reliable standards to determine absolute concentration were not available. We tentatively used the relative sensitivity factors (RSF) of GaN, since these are expected to be similar to those of ScN. Consequently, the actual [H] and [Cl] in Fig. 9 may differ from the true values by a factor of 2–3. However, even if the true value for [Cl] was 10 times larger than our tentative one ($[Cl] = 1.0 \times 10^{18}\,\mathrm{cm}^{-3}$), this is still considerably smaller than that reported by Dismukes *et al*., with $[Cl] = 1.8 \times 10^{20}\,\mathrm{cm}^{-3}$.[32] These results indicate that the corrosion of the reactor materials is efficiently suppressed even at the high growth temperature of 1050 °C, which is substantially higher than those of previous HVPE reports. In addition, our high growth temperature could enhance the desorption of chlorine from the growth surface and favor a low [Cl] in our ScN films.

H. Electrical properties

The carrier concentration dependence of the electron mobility is shown in Fig. 10. The represented data correspond to nominally un-doped samples with various thicknesses (between 0.4–40 μm), using the same growth recipe but different deposition times. The carrier concentration varies within two order of magnitude, no systematical correlation is found between this and the thickness or crystalline

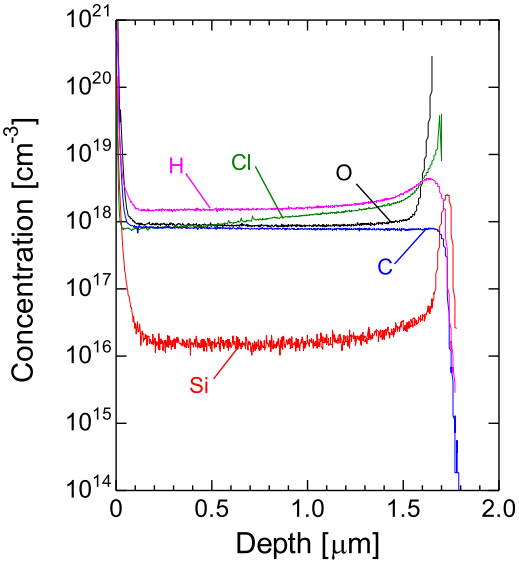

FIG. 9. SIMS depth profile of ScN(100). Note that concentrations of H and Cl are tentative ones calibrated with the RSFs of GaN. Therefore, these values may differ from the true ones by a factor of 2–3.

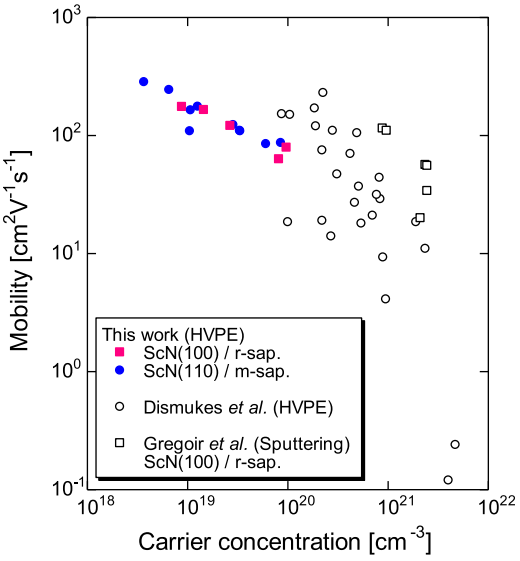

FIG. 10. Carrier concentration dependence of electron mobility.

quality. Clearly, some unknown and uncontrolled factor is dominating the residual carrier concentration. It appears also that there is no significant difference between ScN(100) and ScN(110). The data reported in the literature[29,32] are shown together for the sake of comparison. It is seen that the measured carrier concentrations are substantially lower than the reported ones, and that the electron mobility monotonically increases with decreasing carrier concentration. This can be reasonably explained by assuming a decrease of carrier scattering on ionized donors.

In order to investigate the origin of the residual carrier concentration, we compared the SIMS results between two samples with largely different carrier concentrations (Table II). Here, we denote the samples with high ($n = 8.1 \times 10^{19}$ cm^{-3}) and low ($n = 1.0 \times 10^{19}$ cm^{-3}) carrier concentration as samples A and B, respectively. Again, it should be reminded that [H] and [Cl] are tentative values calibrated with the RSFs of GaN, and therefore these could be different from their true values by a factor of 2–3. Among the impurities listed in Table II, C and O are the only elements whose concentration is higher in sample A. However, the variances between sample A and B are too small to explain the difference in carrier concentration. On the other hand, [Si] and [Cl] are larger in sample B. However, they should act as donor in ScN, and cannot be the cause of the carrier concentration difference. [H] is also greater in sample B, but its contribution to the electrical properties of ScN is still unknown. However, also in this case, the difference is too small to account for the carrier concentration divergence even if the true values of [H] were 10 times larger than our tentative values. These results suggest that the dominant donor species in our ScN films are not related to the elements listed in Table II. According to Smith *et al.*, nitrogen vacancies can also act as donors.[3] In order to clarify the actual origin of the residual carrier concentration, further investigations are required.

TABLE II. Comparison of impurity concentrations (cm^{-3}) in ScN films with largely different free electron concentrations.

Element	Sample A $n = 8.1 \times 10^{19}$ (cm^{-3})	Sample B $n = 1.0 \times 10^{19}$ (cm^{-3})
H	$(1.6 \times 10^{18})^a$	$(2.3 \times 10^{18})^a$
C	7.9×10^{17}	6.2×10^{17}
O	8.8×10^{17}	2.9×10^{17}
Si	1.6×10^{16}	5.4×10^{16}
Cl	$(1.0 \times 10^{18})^a$	$(1.7 \times 10^{18})^a$

[a]Tentative values, calibrated with the RSFs of GaN.

IV. SUMMARY

Single crystalline ScN(100) and ScN(110) films are successfully grown on r- and m-plane sapphire substrates by HVPE. The growth rate has a peak for the partial pressures of both HCl and NH_3, and the maximum growth rate was 5 μm/h. All the single crystalline samples had mirror-like surface with hillocks, which were visible by Nomarski microscope and SEM. The hillock size increased with increasing the film thickness. The surface of ScN(100) appeared to be smoother than that of ScN(110), which can be originated from the difference in surface diffusion barrier. The tilt and twist angles for both ScN(100) and ScN(110) drastically improved with increasing the film thickness. The structural quality of ScN(110) was better than that of ScN(100) probably due to the better lattice matching to sapphire substrates. The optical band gap was estimated to be 2.06 eV through transmittance and reflectance measurements. The N/Sc composition ratio was 1.01 ± 0.10, i.e., stoichiometric within the accuracy of RBS. EDX and SIMS revealed that impurity concentrations were successfully reduced compared to the reported values. This was achieved by a home-made corrosion-resistant HVPE reactor and a high growth temperature. Our nominally un-doped samples show n-type conductivity similar to the reported results. However, the residual carrier concentration was markedly lower, ranging between 10^{18}-10^{20} cm^{-3}. The carrier mobility increased with decreasing the carrier concentration, and reached 284 cm^2 V^{-1} s^{-1} at $n = 3.7 \times 10^{18}$ cm^{-3}, which is the highest value ever reported. It was found that the electrical properties (carrier concentration and mobility) are not directly affected by the structural quality. Additionally, there is no clear evidence of a correlation between the impurity concentrations of H, C, O, Si, and Cl and the electrical properties. Further work is required to clarify the dominant origin of the residual donors in order to enable the conductivity control.

ACKNOWLEDGMENTS

This work was partly supported by a Grant-in-Aid for Young Scientists (B) No. 25790050 from Japan Society for the Promotion of Science (JSPS). Part of this work was conducted for implementing the Ministry of Education, Culture, Sports, Science and Technology (MEXT) Elements Strategy Initiative to Form Core Center of Japan. The authors wish to thank Dr. Takaaki Mano for his great help in measuring X-ray pole figures.

[1]M. A. Moram, Z. H. Barber, C. J. Humphreys, T. B. Joyce, and P. R. Chalker, J. Appl. Phys. **100**, 023514 (2006).
[2]D. Gall, I. Petrov, N. Hellgren, L. Hultman, J. E. Sundgren, and J. E. Greene, J. Appl. Phys. **84**, 6034 (1998).

[3]A. R. Smith, H. A. AL-Brithen, D. C. Ingram, and D. Gall, J. Appl. Phys. **90**, 1809 (2001).
[4]H. A. Al-Brithen, A. R. Smith, and D. Gall, Phys. Rev. B **70**, 045303 (2004).
[5]X. Bai and M. E. Kordesch, Appl. Surf. Sci. **175–176**, 499 (2001).
[6]M. A. Moram, M. J. Kappers, Z. H. Barber, and C. J. Humphreys, J. Cryst. Growth **298**, 268 (2007).
[7]M. J. Kappers, M. A. Moram, Y. Zhang, M. E. Vickers, Z. H. Barber, and C. J. Humphreys, Physica B **401–402**, 296 (2007).
[8]M. A. Moram, Y. Zhang, M. J. Kappers, Z. H. Barber, and C. J. Humphreys, Appl. Phys. Lett. **91**, 152101 (2007).
[9]M. A. Moram, M. J. Kappers, T. B. Joyce, P. R. Chalker, Z. H. Barber, and C. J. Humphreys, J. Cryst. Growth **308**, 302 (2007).
[10]M. E. Little and M. E. Kordesch, Appl. Phys. Lett. **78**, 2891 (2001).
[11]C. Constantin, H. A. Al-Brithen, M. B. Haider, D. Ingram, and A. R. Smith, Phys. Rev. B **70**, 193309 (2004).
[12]C. Constantin, M. B. Haider, D. Ingram, A. R. Smith, N. Sandler, K. Sun, and P. Ordejón, J. Appl. Phys. **98**, 123501 (2005).
[13]A. B. Fredj, Y. Oussaifi, N. Bouarissa, and M. Said, Phys. Status Solidi B **243**, 2780 (2006).
[14]S. Zerroug, F. A. Sahraoui, and N. Bouarissa, J. Appl. Phys. **103**, 063510 (2008).
[15]M. A. Moram, Y. Zhang, T. B. Joyce, D. Holec, P. R. Chalker, P. H. Mayrhofer, M. J. Kappers, and C. J. Humphreys, J. Appl. Phys **106**, 113533 (2009).
[16]S. M. Knoll, S. Zhang, T. B. Joyce, M. J. Kappers, C. J. Humphreys, and M. A. Moram, Phys. Status Solidi A **209**, 33 (2012).
[17]F. Perjeru, X. Bai, M. I. Ortiz-Libreros, R. Higgins, and M. E. Kordesch, Appl. Surf. Sci. **175–176**, 490 (2001).
[18]S. Kerdsongpanya, N. V. Nong, N. Pryds, A. Žukauskaitė, J. Jensen, J. Birch, J. Lu, L. Hultman, G. Wingqvist, and P. Eklund, Appl. Phys. Lett. **99**, 232113 (2011).
[19]P. V. Burmistrova, J. Maassen, T. Favaloro, B. Saha, S. Salamat, Y. Rui Koh, M. S. Lundstrom, A. Shakouri, and T. D. Sands, J. Appl. Phys. **113**, 153704 (2013).
[20]H. A. Al-Brithen, H. Yang, and A. R. Smith, J. Appl. Phys. **96**, 3787 (2004).
[21]A. Herwadkar and W. R. L. Lambrecht, Phys. Rev. B **72**, 235207 (2005).
[22]M. Akiyama, K. Kano, and A. Teshigahara, Appl. Phys. Lett. **95**, 162107 (2009).
[23]M. Akiyama, K. Umeda, A. Honda, and T. Nagase, Appl. Phys. Lett. **102**, 021915 (2013).
[24]V. Ranjan, L. Bellaiche, and E. J. Walter, Phys. Rev. Lett. **90**, 257602 (2003).
[25]H. Al-Brithen and A. R. Smith, Appl. Phys. Lett. **77**, 2485 (2000).
[26]H. Al-Brithen, E. M. Trifan, D. C. Ingram, A. R. Smith, and D. Gall, J. Cryst. Growth **242**, 345 (2002).
[27]M. A. Moram, T. B. Joyce, P. R. Chalker, Z. H. Barber, and C. J. Humphreys, Appl. Surf. Sci. **252**, 8385 (2006).
[28]M. A. Moram, S. V. Novikov, A. J. Kent, C. Nörenberg, C. T. Foxon, and C. J. Humphreys, J. Cryst. Growth **310**, 2746 (2008).
[29]J. M. Gregoire, S. D. Kirby, G. E. Scopelianos, F. H. Lee, and R. B. Dover, J. Appl. Phys. **104**, 074913 (2008).
[30]T. Ohgaki, K. Watanabe, Y. Adachi, I. Sakaguchi, S. Hishita, N. Ohashi, and H. Haneda, J. Appl. Phys. **114**, 093704 (2013).
[31]J. P. Dismukes, W. M. Yim, J. J. Tietjen, and R. E. Novak, RCA Rev. **31**, 680 (1970).
[32]J. P. Dismukes, W. M. Yim, and V. S. Ban, J. Cryst. Growth **13/14**, 365 (1972).
[33]J. J. Tietjen and J. A. Amic, J. Electrochem. Soc. **113**, 724 (1966).
[34]Y. Oshima, T. Eri, M. Shibata, H. Sunakawa, K. Kobayashi, T. Ichihashi, and A. Usui, Jpn. J. Appl. Phys., Part 2 **42**, L1 (2003).
[35]K. Motoki, T. Okahisa, N. Matsumoto, M. Matsushima, H. Kimura, H. Kasai, K. Takemoto, K. Uematsu, T. Hirano, M. Nakayama, S. Nakahata, M. Ueno, D. Hara, Y. Kumagai, A. Koukitu, and H. Seki, Jpn. J. Appl. Phys., Part 2 **40**, L140 (2001).
[36]J. H. Edgar, T. Bohnen, and P. R. Hageman, J. Cryst. Growth **310**, 1075 (2008).
[37]K. J. Hubbard and D. G. Schlom, J. Mater. Res. **11**, 2757 (1996).
[38]L. D. Polyachenok, K. Nazarov, and O. G. Polyachenok, Z. Fiz. Khim **52**, 1767 (1978).
[39]Y. B. Patrikeev, V. A. Morozova, G. P. Dudchik, O. G. Polyachenok, and G. I. Novikov, Russian J. Phys. Chem. **47**, 266 (1973).
[40]W. Lengauer, J. Solid State Chem. **76**, 412 (1988).
[41]K. Fujito, S. Kubo, H. Nagaoka, T. Mochizuki, H. Namita, and S. Nagao, J. Cryst. Growth **311**, 3011 (2009).
[42]D. Gall, I. Petrov, L. D. Madsen, J. E. Sundgren and J. E. Greene, J. Vac. Sci. Technol. A **16**, 2411 (1998).
[43]M. A. Moram, Z. H. Barber, and C. J. Humphreys, Thin Solid Films **516**, 8569 (2008).